Journal of Applied Electrochemistry **30**: 1005–1014, 2000.

Two-dimensional numerical modelling of a direct methanol fuel cell

A.A. KULIKOVSKY*
Institute for Materials and Processes in Energy Systems (IWV-3), Research Center "Jülich", D-52425 Jülich, Germany
*(*address for correspondence: Moscow State University, Research Computing Center (NIVC), 119899 Moscow, Russia, e-mail: akul@srcc.msu.su)*

Received 19 July 1999; accepted in revised form 10 April 2000

Key words: DMFC, methanol crossover, numerical modelling

Abstract

The results of a numerical simulation of a direct methanol fuel cell (DMFC) with liquid methanol feed are presented. A two-dimensional numerical model of a DMFC is developed based on mass and current conservation equations. The velocity of the liquid is governed by gradients of membrane phase potential (electroosmotic effect) and pressure. The results show that, near the fuel channel, transport of methanol is determined mainly by the pressure gradient, whereas in the active layers, and in the membrane, diffusion transport dominates. 'Shaded' zones, where there is a lack of methanol, are formed in front of the current collectors. The results reveal a strong influence of the hydraulic permeability of the backing layer K_p^{BL} on methanol crossover through the membrane. If the value of K_p^{BL} is comparable to that of the membrane and active layers, electroosmotic effects lead to the formation of an inverse pressure gradient. The flux of liquid driven by this pressure gradient is directed towards the anode and reduces methanol crossover.

1. Introduction

The direct methanol fuel cell (DMFC) is an attractive source of power for applications such as vehicles. Although classical hydrogen–oxygen fuel cells exhibit superior performance, methanol has a much higher energy density and is much easier to store and transport.

At the anode of a DMFC methanol ionization occurs on the catalyst surface according to

$$CH_3OH + H_2O \rightarrow CO_2 + 6\,H^+ + 6\,e^- \quad (1)$$

Protons then move to the cathode, where they react with oxygen:

$$\frac{3}{2}\,O_2 + 6\,H^+ + 6\,e^- = 3\,H_2O \quad (2)$$

The overall reaction in the cell is

$$CH_3OH + \frac{3}{2}\,O_2 \rightarrow CO_2 + 2\,H_2O \quad (3)$$

that is the byproducts are ecologically harmless CO_2 and water. This is another reason why DMFC has received so much attention during the past decade.

To our knowledge two models of a DMFC have been published: by Wang and Savinell [1] and by Scott et al. [2, 3]. These models stem from the models of the conventional, hydrogen–oxygen polymer electrolyte fuel cell (PEFC) [4, 5]. All these models are one-dimensional; that is the transport processes are considered across the cell only. However, the presence of fuel and gas channels on both sides of the cell leads to the formation of complex two-dimensional fields of electrical potential and reactant concentration. This has been shown in [6] for the DMFC with gas methanol feed.

Two types of DMFC are under investigation. In one of these methanol is supplied to the anode under elevated temperature (typically 110–130 °C) in gaseous form. The other type of cell works at low temperature (typically 80 °C) with liquid methanol as fuel. Both types have advantages and disadvantages. Methanol ionization proceeds better in the high temperature cell. At high current densities, however, this cell suffers from membrane drying, which leads to degradation in cell performance. The low temperature cell exhibits lower anode activity, but is fully hydrated and hence has no limitations related to membrane drying.

One of the most essential problems in the creation of low-cost and effective DMFCs is methanol permeation through the membrane. This process leads to 'parasitic' methanol ionization in the cathode catalyst layer. Ions and electrons produced in this reaction do not contribute to current generation. Instead, when they recombine, they consume oxygen in Reaction 2.

A two-dimensional numerical model of a high temperature DMFC with gas feed was developed earlier [6].

In the present work a two-dimensional model of a DMFC with liquid methanol feed is described. The aim of this work is to elucidate the mechanism of liquid methanol transport in the cell and to find ways of reducing methanol crossover.

2. The model

2.1. *General assumptions*

The model is based on the following assumptions:

(i) There are two different types of pores in the catalyst and backing layers: 'gas' (hydrophobic) pores and 'liquid' (hydrophilic) pores and there are no connections between the different pore types. At the anode side CO_2 is created in the gas phase and is removed via hydrophobic pores, whereas liquid moves in the hydrophilic pores. At the cathode side the components supplied from the air channel (N_2, O_2 and water vapour) are transported in the hydrophobic pores.

(ii) In practice methanol is mixed with water in the proportion 1 M:55 M. The large amount of excess water allows variations in liquid density caused by the reaction at the anode to be neglected.

(iii) At the cathode side electrochemical reaction consumes gaseous oxygen and produces liquid water. This water is accounted for in the overall liquid balance in the cell.

(iv) At the cathode side, in the hydrophobic pores water saturation conditions exist; that is the pressure of water vapour depends only on temperature.

(v) The pressure of the liquid mixture is kept fixed in the channels.

(iv) The pressure of gas at the cathode side is constant.

These assumptions mean that, to a first approximation, mass transfer between liquid and gas phases is neglected.

A sketch of the cell is shown in Figure 1. The fuel and oxygen are supplied to the electrodes through the channels made in the highly conductive current collectors. Usually a DMFC assembly has many parallel channels on both sides, so the sketch in Figure 1 represents an elementary part of the cell. The methanol and oxygen are transported through the backing (or gas diffusion) layers (DA and DC, respectively) to the active layers (RA and RC), where electrochemical reactions occur.

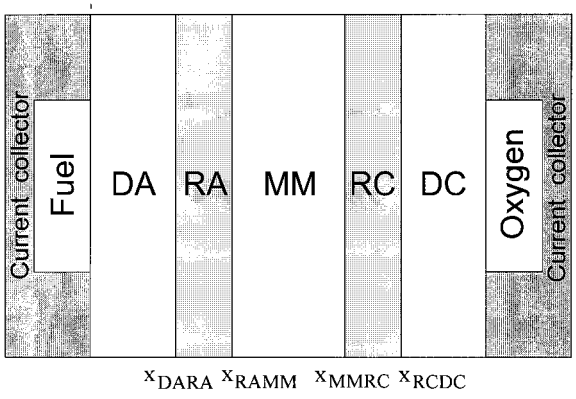

Fig. 1. Sketch of conventional cell. Abbreviations: (DA), (DC) anode, cathode diffusion layers, resp.; (RA), (RC) anode, cathode catalyst layers, resp.; (MM) membrane. Notations of positions of interfaces are shown beneath.

The catalyst layer is usually made by hot pressing of a liquid polymer electrolyte, loaded with catalyst powder into the carbon cloth. This gives a thin (about 10 μm) catalyst layer on one side of the cloth. The rest of the cloth volume serves as a backing (diffusion) layer. Reactions 1 and 2 occur at the surface of catalyst particles and involve protons, electrons and neutral molecules. These three types of species are transported through different avenues to the reaction sites: protons move through the electrolyte, electrons through the carbon threads and molecules through the voids. The electrode is a tortuous mixture of these avenues. This structure is usually described as a uniform continuous medium with some mean transport parameters associated with the each type of species. In our model we use this approach.

2.2. *Potentials*

Following the concept of mean parameters we introduce the electrical potentials of the membrane and carbon phases. The first potential governs the motion of protons and the second that of electrons. Let the potential of membrane phase be φ_m and the potentials of the carbon phase at the anode and the cathode be φ_a and φ_c, respectively. The three potentials obey the following equations:

$$\nabla \cdot (\sigma_m \nabla \varphi_m) = \begin{cases} -R_a & x_{DARA} < x \leqslant x_{RAMM} \\ 0 & x_{RAMM} < x < x_{MMRC} \\ R_c & x_{MMRC} \leqslant x < x_{RCDC} \end{cases} \tag{4}$$

$$\nabla \cdot (\sigma_n \nabla \varphi_a) = \begin{cases} 0 & x < x_{DARA} \\ R_a & x_{DARA} \leqslant x < x_{RAMM} \end{cases} \tag{5}$$

$$\nabla \cdot (\sigma_n \nabla \varphi_c) = \begin{cases} -R_c & x_{MMRC} < x \leqslant x_{RCDC} \\ 0 & x_{RCDC} < x \end{cases} \tag{6}$$

where σ_m, σ_n are the conductivities of membrane and carbon phases, respectively, and R_a and R_c are rates of electrochemical reaction at the anode and the cathode catalyst layers. Explicit expressions for R_a and R_c are presented in the following Section. The symbols x_{DARA}, x_{RAMM}, x_{MMRC}, x_{RCDC} denote the position of interfaces (Figure 1).

It is assumed that the conductivity of the carbon phase, σ_n, is constant. Sometimes carbon cloth with anisotropic conductivity is used: the 'in plane' and 'normal to plane' conductivities may differ significantly. We do not consider such a situation here. Our numerical

scheme, however, allows this effect to be taken into account.

2.3. *Reactions rates*

Methanol ionization (Reaction 1) is a complicated multistage process, which includes formation of adsorbate on the catalyst surface. Under different overpotentials the rate determining step may be different. The reaction rate also depends on the crystalline structure of the catalyst. Strictly speaking the reaction rate may not follow a simple Tafel expression: under different conditions the functional form of this rate can vary. This issue has been discussed in more detail in [6], where the relevant references can be found. Similar arguments are valid for the oxygen side. Nevertheless, Tafel equations for the rates of both anodic and cathodic reactions were used. The expressions in this Section are a fit of available experimental data, as discussed in [6], and correspond to certain specific methods of catalyst layer preparation.

The rate of charged particle generation (A cm^{-3}) in Reaction 1 is given as

$$R_a = i^0_{a\,ref}\left(\frac{p_M}{p_{M\,ref}}\right)\exp\left(\frac{\alpha_a F}{RT}(\varphi_a - \varphi_m)\right) \tag{7}$$

where F and R are the Faraday number and gas constant, respectively, $\alpha_a = 0.5$ (Table 1) is the anodic transfer coefficient.

The rate of charged particle loss in Reaction 2 (A cm^{-3}) is given as

$$R_c = i^0_{c\,ref}\sqrt{\frac{c_{O_2}}{c_{O_2\,ref}}}\exp\left(\frac{\alpha_c F}{RT}(\varphi_m - \varphi_c)\right) \tag{8}$$

Following Bernardi and Verbrugge [7] the 'square root' dependence of R_c on oxygen concentration and $\alpha_c = 2$ (Table 1) were adopted.

Table 1. Conditions and parameters at the anode and the cathode

	Anode side	Cathode side
Pressure/atm	3.0	2.0
Oxygen number density fraction in the channel*		0.77
Water vapour number density fraction in the channel		0.23
Nitrogen number density fraction in the channel		0.0
Methanol content in the channel/mol	1×10^{-3}	
Liquid water content in the channel/mol	55×10^{-3}	
$c_{O_2\,ref}$/mol cm^{-3}		3.18×10^{-5}
$p_{M\,ref}$/atm	0.97	
i^0_{ref}/A cm^{-3}	1.0	1.0×10^{-5}
α	0.5	2.0

* Number density fraction is n_x/n, where n_x is number density of species x and n total number density

Table 2. Parameters, common for the anode and the cathode

Cell temperature/°C	80
Mean pore radius in backing layer $\langle r\rangle$/cm	10^{-5}
Mean pore radius in catalyst layer $\langle r\rangle$/cm	10^{-6}
Proton diffusion coeff. D_H/cm^2 s^{-1}	4.5×10^{-5}
Proton concentration c_H/mol cm^{-3}	1.2×10^{-3}
ϵ_M in Equation 17	0.2
Hydraulic permeability of backing layer K_p^{BL}/cm^2	3.03×10^{-12}
Hydraulic permeability of membrane K_p^M/cm^2	1.8×10^{-14}
Electrokinetic permeability of membrane K_φ^M/cm^2	7.18×10^{-16}
Correction factor ε^M in Equations 20 and 21	0.5
ϵ in Equation 22	0.12
ψ in Equation 23	0.156
Catalyst layer thickness/cm	0.001
Backing layer thickness/cm	0.01
Membrane thickness/cm	0.002

Methanol, which penetrates through the membrane to the cathode catalyst layer, is consumed there in a parasitic 'anodic' reaction (Reaction 1), whose rate is given by Reaction 7 with the potential difference $\varphi_m - \varphi_c$:

$$R^*_c = i^0_{a\,ref}\left(\frac{p_M}{p_{M\,ref}}\right)\exp\left(\frac{\alpha_a F}{RT}(\varphi_m - \varphi_c)\right) \tag{9}$$

2.4. *Pressure of liquid*

The density of the liquid is assumed constant. Moreover, as methanol is a small fraction of the mixture, changes in flux of liquid caused by the anodic reaction may be neglected. However, a significant amount of water is produced in the cathodic reaction. The velocity of the liquid mixture, $\mathbf{v}$, is then defined by the mass conservation equation

$$\rho\nabla\cdot\mathbf{v} = \begin{cases} R^w_c & x_{MMRC} \leqslant x \leqslant x_{RCDC} \\ 0 & \text{otherwise} \end{cases} \tag{10}$$

where R^w_c is the rate of water production in the cathodic reaction and ρ is the liquid density.

We assume that the velocity of the liquid is related to the gradients of membrane phase potential φ_m and pressure p (Schlögl's equation):

$$\mathbf{v} = -\frac{K_\varphi}{\mu}c_H F\nabla\varphi_m - \frac{K_p}{\mu}\nabla p \tag{11}$$

This equation takes into account the two forces acting on the fluid: drag caused by ion movement under the electric field (electroosmotic effect) and the pressure gradient (Poiseuille flow in hydrophilic pores). Here μ is fluid viscosity, K_φ and K_p are electrokinetic and hydraulic permeabilities, respectively and c_H is the proton concentration in the membrane phase.

The system of equations (Equations 10, 11 and 4) defines three unknown functions $\mathbf{v}$, p and φ_m. The velocity $\mathbf{v}$ can be eliminated by taking the divergence of Equation 11:

$$\mu\nabla\cdot\mathbf{v} = -c_H F\nabla\cdot\left(K_\varphi\nabla\varphi_m\right) - \nabla\cdot\left(K_p\nabla p\right) = \frac{\mu}{\rho}R_c^w$$

or

$$\nabla\cdot\left(K_p\nabla p\right) = -c_H F\nabla\cdot\left(K_\varphi\nabla\varphi_m\right) - \frac{\mu}{\rho}R_c^w \tag{12}$$

Equation 12 shows that there are two volume sources of pressure in the electrode: electroosmotic flux and water production in the cathode catalyst layer.

2.5. *Methanol transport*

Solving Equation 12 under given φ_m gives the pressure distribution in the cell. Equation 11 then gives the velocity of liquid methanol. Since the methanol concentration in water is small, the methanol flux is proportional to the concentration gradient (Fick's law) plus the flux caused by the flow of liquid as a whole. The continuity equation for the molar concentration of methanol c_M in the anode catalyst layer is, therefore,

$$\nabla\cdot(-D_M\nabla c_M + \mathbf{v}c_M) = -\frac{S_M}{nF}R_a, \quad x_{DARA} \leqslant x \leqslant x_{RAMM} \tag{13}$$

where D_M is the diffusion coefficient of methanol in the mixture, R_a is the rate of charged particle production and $S_M = 1$ is the stoichiometric coefficient.

Similarly, in the cathode catalyst layer the methanol concentration is governed by Equation 13, where the rate of the 'parasitic' reaction (Reaction 9) R_c^* should be used instead of R_a. In the backing layer and in the membrane there are no source or loss of methanol. Therefore, we have

$$\nabla\cdot(-D_M\nabla c_M + \mathbf{v}c_M) = \begin{cases} 0, & 0 < x < x_{DARA} \\ -\frac{S_M}{nF}R_a, & x_{DARA} \leqslant x \leqslant x_{RAMM} \\ 0, & x_{RAMM} < x < x_{MMRC} \\ -\frac{S_M}{nF}R_c^*, & x_{MMRC} \leqslant x < x_{RCDC} \end{cases} \tag{14}$$

It is assumed that at $x = x_{RCDC}$ $c_M = 0$.

2.6. *Transport of gases on the cathode side*

It is assumed that water saturation conditions exist in the hydrophobic pores on the cathode side. This means that in these pores there is no flux of water vapour. Since nitrogen does not participate in the cathodic reaction, the flux of nitrogen is also zero.

In [8] the model of gas flow in the cathode compartment was developed. When the fluxes of water vapour and nitrogen are zero this model reduces to a single equation for the relative oxygen concentration, ξ_{O_2}:

$$\nabla\cdot\left(-c\nabla\xi_{O_2}\right) = \mathbf{G}_{O_2}\cdot\nabla\left(\frac{1}{D^K_{O_2}} + \frac{\xi_{N_2}}{D_{N_2O_2}} + \frac{\xi_w}{D_{O_2w}}\right) - \left(\frac{1}{D^K_{O_2}} + \frac{\xi_{N_2}}{D_{N_2O_2}} + \frac{\xi_w}{D_{O_2w}}\right)\frac{S_{O_2}}{nF}(R_c + R_c^*) \tag{15}$$

where the flux $\mathbf{G}_{O_2}$ is defined by

$$\left(\frac{1}{D^K_{O_2}} + \frac{\xi_{N_2}}{D_{N_2O_2}} + \frac{\xi_w}{D_{O_2w}}\right)\mathbf{G}_{O_2} = -c\nabla\xi_{O_2} \tag{16}$$

Here $\xi_k \equiv c_k/c$ is the relative molar concentration of the kth component, c is the total molar concentration of the mixture and subscripts 'N_2', 'O_2' and 'w' stand for oxygen, nitrogen and water vapour, respectively. The values of ξ_{N_2} and ξ_w are constant and are defined by the external conditions. The symbols D^K stand for Knudsen diffusion coefficients; D's without superscript denote binary diffusion coefficients.

Oxygen is consumed in Reaction 8 (the term R_c) and in the parasitic reaction with the products of methanol ionization in the cathode catalyst layer (the term R_c^*).

2.7. *Boundary conditions and numerical method*

The model consists of six conservation equations. Equations 4–6 govern potentials, Equation 12 pressure, Equation 14 methanol concentration and Equation 15 oxygen concentration at the cathode. Boundary conditions for the problem are shown in Figure 2. Below and above the channels the carbon phase potentials are fixed by the highly conductive current collectors. At the channel surfaces the normal component of electron current is zero: $\partial\varphi_{a,c}/\partial x = 0$. On both sides of membrane the electronic current densities are also zero.

Equation 4 for membrane phase potential is solved in the domain $x_{DARA} < x < x_{RCDC}$, where polymer electrolyte exists. On the left and right sides of this domain the normal component of proton current density is zero (Figure 2).

Equation 12 governs the distribution of liquid pressure in the cell. Boundary conditions for this equation are as follows. It is assumed that on both sides of the cell a fixed pressure occurs in the channels. At the surfaces of the current collectors the normal component of fluid velocity is zero, that is $\partial p/\partial x = 0$.

The computational domain covers a part of the cell assembly. Therefore, at $y = 0$ and $y = H$, periodic boundary conditions for all variables are imposed.

Equations 4–6 and 12 were converted to finite difference form using a well-known 5-point approximation formula. The equation for methanol concentration Equation 14 is of convection-diffusion type and is formally analogous to Equation 15. The Scharfetter–Gummel scheme was used for approximation of

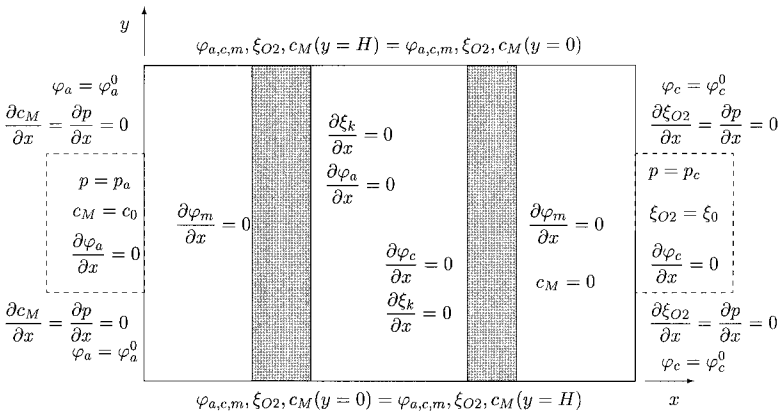

Fig. 2. Boundary conditions for cell with conventional current collectors. Fuel and oxygen channels are depicted by dashed boxes on both sides.

methanol and oxygen fluxes through the surfaces of the computational cell. The detailed description of numerical aspects can be found in [8].

3. Results and discussion

Unless stated otherwise, the parameters listed in Table 1 (base case) were used. The transport coefficients are given in the Appendix.

3.1. *Cell with conventional electrodes*

Figure 3 shows the distributions of concentrations, reactions rates and proton current density (mean current density is 0.4 A cm^{-2}). A peculiarity of the cell with liquid methanol feed is the very low methanol concentration in the catalyst layers in front of the current collectors (in the 'shaded' regions) (Figure 3(a)). The reaction rate in the shaded regions of the anode catalyst layer is five times lower than in front of the fuel channel (Figure 3(b)). Proton current flows mainly in front of the fuel channel (Figure 3(c)). Clearly, one can safely remove catalyst from the shaded regions of the catalyst layer.

Most of the current is generated in front of the fuel channel. This leads to formation of intensive 'torches' of electronic current near the edges of the current collectors (Figure 4). Similar effects have been found in DMFCs with gaseous methanol feed [8]. Physically, the electrons

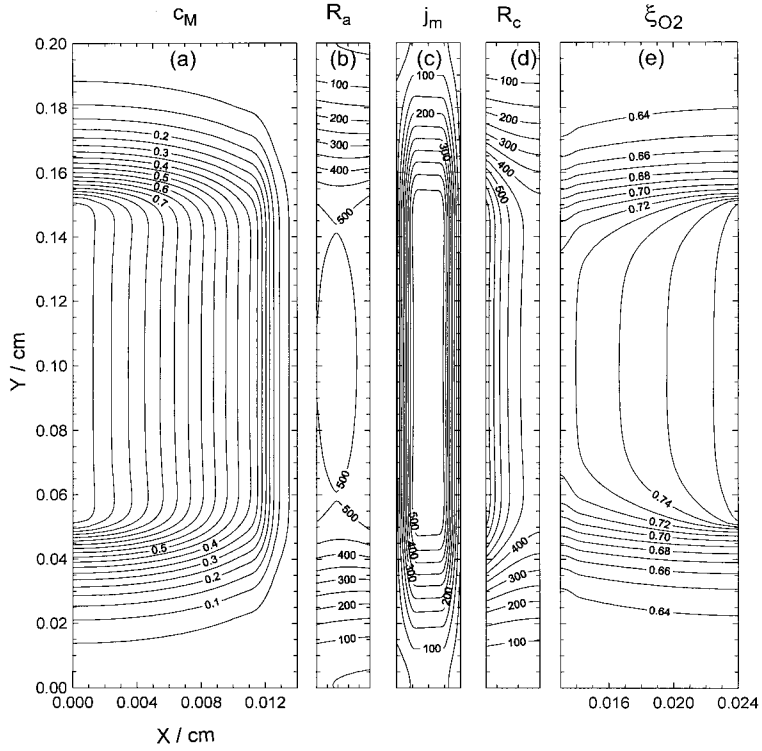

Fig. 3. Contour maps of (a) methanol concentration (10^{-3} mol cm^{-3}), (b) reaction rate in the anode catalyst layer (A cm^{-3}), (c) proton current density (mA cm^{-2}), (d) reaction rate in the cathode catalyst layer (A cm^{-3}) and (e) oxygen relative number density (see Table 1 caption).

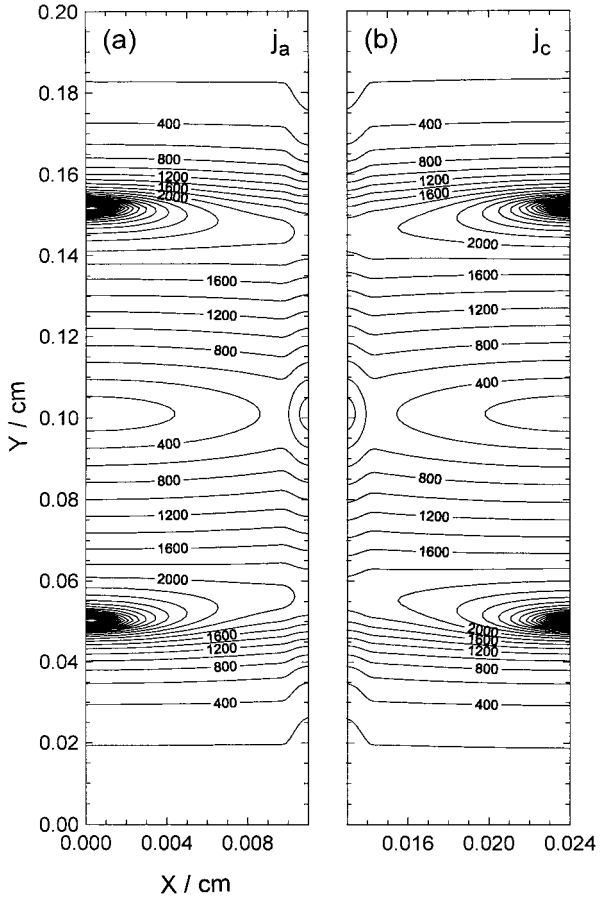

Fig. 4. Contour maps of electron current density (mA cm^{-2}): (a) in anode compartment (backing and catalyst layers) and (b) in cathode compartment.

produced in front of the fuel channel flow to the nearest point of the current collector (i.e., to the edge). The current density at the edges is more than ten times greater than the mean current density which may lead to local overheat.

According to Equation 14, the methanol flux is supported by two processes: convection and diffusion. Figure 5 shows both components of the flux. It is seen that the convective term, $\mathbf{v}c_M$, dominates near the edges of the current collector. In the catalyst layer ($x > 0.01$ cm) the diffusion transport of methanol dominates. The gradient of methanol concentration here is very high and the diffusion flux exceeds the convective flux.

The distribution of pressure in the cell is shown in Figure 6. Due to the electroosmotic flux a 'stair' is formed in the region which includes both catalyst layers and membrane ($0.01 \leqslant x \leqslant 0.014$ cm). The electroosmotic flux tends to invert the sign of the pressure gradient. The inversions, however, do not occur due to the high value of hydraulic permeability of the backing layer K_p^{BL}. In other words, the high value of K_p^{BL} 'transports' the channel boundary conditions for pressure to the boundaries of the catalyst layers. All the pressure gradient is concentrated in the catalyst layers and membrane.

What happens if the hydraulic permeability of backing layer and the permeabilities of catalyst layers and membrane are of the same order? The results of this numerical experiment are described in the next section.

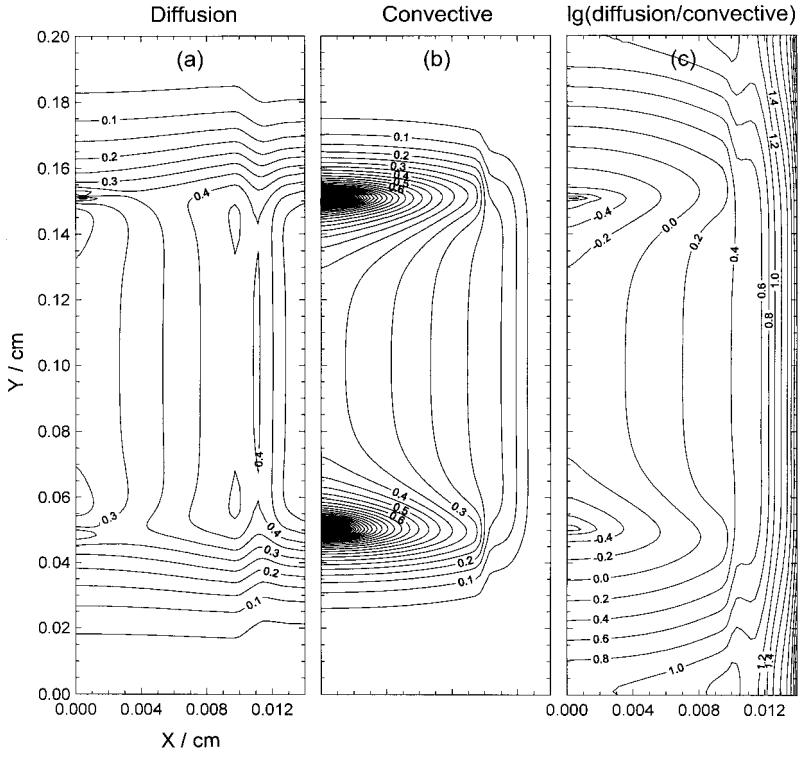

Fig. 5. Absolute values of (a) diffusion $f_D = |D_M \nabla c_M|$ and (b) convective $f_c = |\mathbf{v}c_M|$ components of methanol flux (flux/10^{-6} mol cm^{-2}); (c) log of their ratio, $\log(f_D/f_c)$.

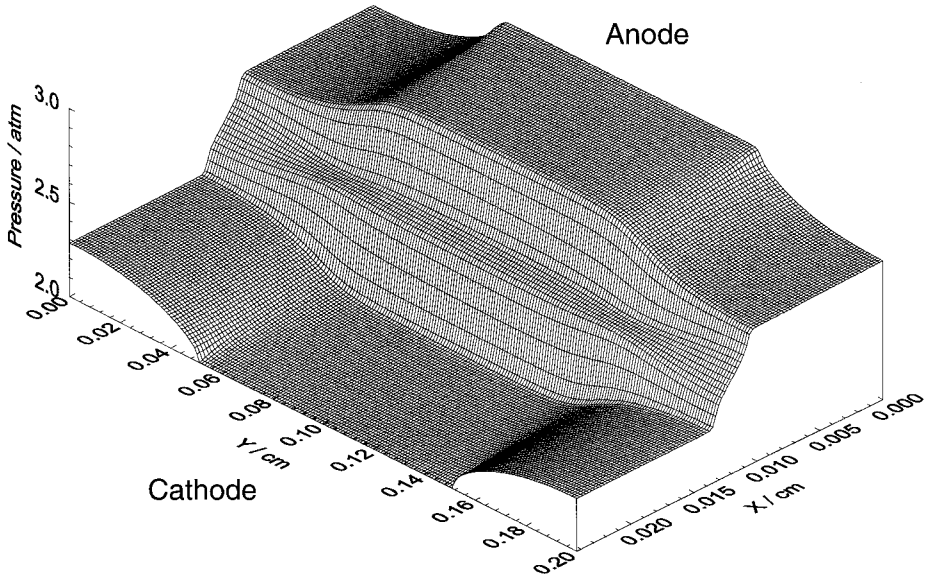

Fig. 6. Pressure distribution in the cell.

3.2. *Quasi one-dimensional cell*

To investigate the role of the hydraulic permeability it is convenient to consider a cell with 'embedded' current collectors, shown in Figure 7. These collectors, described in [6] allow avoidance of the formation of shaded zones. In brief, the idea is to embed current collectors into the backing and catalyst layers thus making collectors on both sides of the cell parallel to the fuel/oxygen flow. This provides uniform (along the y-axis) transport of reactants to the active layers (Figure 7). In this geometry only electrons move along the y-axis, whereas protons, fuel and oxygen move along the x-axis. This type of cell can be called 'quasi one-dimensional'. One-dimensional theories can be verified experimentally using cells of this type.

To accelerate calculations the distance between collectors was taken to be 0.005 cm. This distance is limited by the conductivity of the carbon phase. If the latter is low in the y-direction, there would be ohmic losses associated with the electron transport to the current collectors. In practice this distance may be about 1 cm or more.

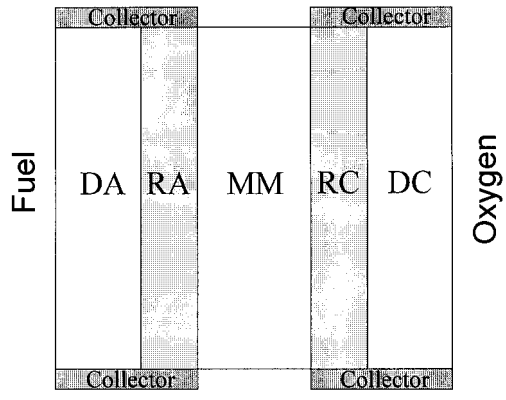

Fig. 7. Sketch of cell with embedded current collectors. Notations same as Figure 1.

Hydraulic permeabilities of the backing layer, catalyst layers and membrane are different, as described in the Appendix. Only the permeability of the backing layer K_p^{BL} was changed. Typically, the carbon cloth has K_p^{BL} of order $10^{-12}\,\mathrm{cm}^2$. We reduce this value by two orders of magnitude (Figure 8). The value of $K_p^{BL} = 3.03 \times 10^{-14}\,\mathrm{cm}^2$ is comparable to permeabilities of the catalyst layer and membrane (Figure 8).

Figure 9 shows the results of this experiment. The curve for $400\ \mathrm{mA\ cm}^{-2}$ in Figure 9(a) displays the formation of the 'stair' on the pressure profile in case when K_p^{BL} is high ($3.03 \times 10^{-12}\,\mathrm{cm}^2$) (cf. Figure 6).

The situation changes dramatically when K_p^{BL} is low ($3.03 \times 10^{-14}\,\mathrm{cm}^2$, Figure 9(b)). In this case, at low current density, the pressure gradient caused by the boundary conditions is distributed uniformly across the cell thickness. Therefore, the pressure gradient across the membrane and catalyst layers is essentially lower than in the case of high K_p^{BL}. The electroosmotic flux is now able to change the sign of the pressure gradient. Even at low current density, due to that flux, the pressure in the cathode catalyst layer becomes higher than the pressure in the anode catalyst layer and an inverse pressure gradient arises (Figure 9(b)). The higher the current density, the more pronounced is the effect.

The inverse pressure gradient reduces the methanol crossover. This gradient forces liquid to move in the opposite direction, towards the anode. The convective flux of methanol $\mathbf{v}c_M$ is, therefore, directed opposite to the diffusion flux and the overall flux of methanol through the membrane diminishes.

Figure 10(a) shows a comparison of methanol fluxes through the membrane for cases of high and low hydraulic permeability. With low K_p^{BL} the methanol crossover decreases when the mean current density in

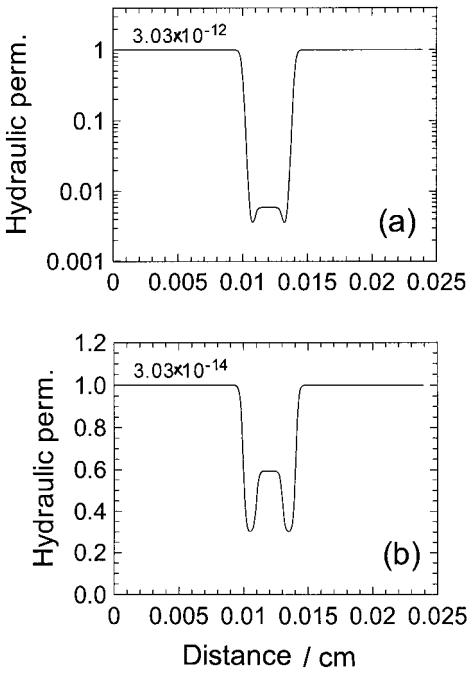

Fig. 8. Profiles of dydraulic permeability along x-axis. Plotted values normalized to permeability in backing layer (shown above each curve). (a) Base case, (b) K_p^{BL} is two orders of magnitude lower than the base case.

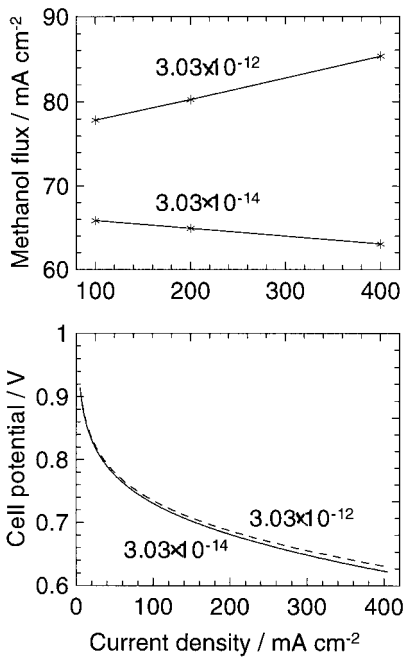

Fig. 10. (a) Methanol flux (mA cm^{-2}), which permeates through membrane for the two indicated values of hydraulic permeability of backing layer (cm^2), (b) voltage–current curves for same values of hydraulic permeability.

the cell increases. The effect is clear: with higher current density the electroosmotic flux increases, the pressure of liquid in the cathode catalyst layer increases and this leads to a growth of inverse convective flux of methanol.

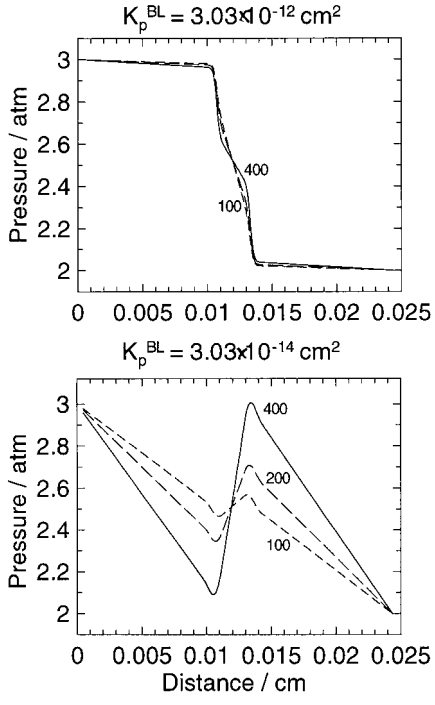

Fig. 9. Pressure profiles along x-axis for the two indicated values of hydraulic permeability of backing layers. Curves are plotted for the three values of mean current density in cell: 100, 200 and 400 mA cm^{-2}.

Figure 10(b) shows the voltage–current curves for both permeabilities K_p^{BL}. The two curves are almost identical. In the case of low K_p^{BL} the voltage loss due to deterioration of liquid transport through the cell is compensated by reduction in methanol crossover. Nevertheless, because of the smaller losses of methanol the low K_p^{BL} is beneficial.

Figure 11 shows the dependence of methanol crossover flux on current density for various methanol concentrations under constant (low) K_p^{BL} value. The model predicts that for $c_M \leqslant 2$ M the crossover decreases with increase in current density. For $c_M > 2$, however, the crossover increases with increase in current density. At high c_M the diffusion flux of methanol cannot be compensated by the inverse pressure gradient for a

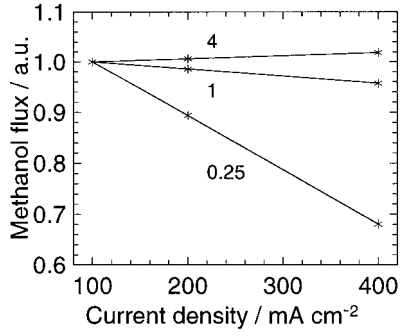

Fig. 11. Dependence of methanol crossover flux on current density in cell for the three indicated values of methanol concentration (M). In all cases $K_p^{BL} = 3.03 \times 10^{-14}$ cm^2.

realistic range of current densities. This behaviour corresponds to experimental observations [9].

Scott et al. [3] demonstrated an essential improvement in cell performance under elevated gas pressure on the cathode side. The effect was attributed in [3] to the reduction of methanol crossover. In more exact terms, the effect can be attributed to the role of the inverse pressure gradient.

4. Conclusions

A two-dimensional simulation of a direct methanol fuel cell with liquid methanol feed was performed. The results show the following:

(i) Methanol-depleted (shaded) regions are formed in the catalyst layer in front of the current collectors. Most of the current is produced opposite the fuel channel.
(ii) 'Torches' of high electron current density are formed near the edges of the current collectors. The current density in these torches exceeds the mean current density in the cell by more than a factor of ten. This may lead to local overheat.
(iii) Under high hydraulic permeability of the backing layer the main mechanism of methanol transport through the catalyst layers and membrane is diffusion.
(iv) If the hydraulic permeability of the backing layer is comparable to that of the catalyst layer and membrane, the electroosmotic effect produces an inverse pressure gradient across the membrane and active layers. This inverse gradient reduces methanol crossover through the membrane. At low concentrations of methanol increase in current density reduces the crossover. This behavior is in qualitative agreement with recent experimental observations [9].

Acknowledgements

The author is grateful to Prof. A.A. Kornyshev and to Dr. J. Divisek for many stimulating discussions. He also acknowledges the assistance of Prof. A.A. Wragg with the English composition of this paper.

Appendix: Transport coefficients

The conductivity of the membrane phase was estimated using the Einstein relation

$$\sigma_m = \epsilon_M \frac{F^2}{RT} D_H c_H \tag{17}$$

where D_H is proton diffusion coefficient, c_{H} proton concentration in the membrane and ϵ_M a correction factor. With the parameters listed in Table 1 this gives $\sigma_m \simeq 0.034\,\Omega^{-1}\,\mathrm{cm}^{-1}$. The conductivities of membrane phase in the catalyst layer and in the bulk membrane were taken to be the same.

Equation 14 contains the *diffusion coefficient of methanol* in water. The water fills the hydrophilic pores in the backing and catalyst layers and exists in the membrane. The process of methanol diffusion transport through the water-filled membrane involves complicated and still poorly understood physics. In simulations the experimental data of [9] were used. These data were approximated by a function

$$D_M^M = 4.012 \times 10^{-9} \exp(0.024312T) \tag{18}$$

where T is temperature in Kelvin. Here D_M^M (in $\mathrm{cm}^2\,\mathrm{s}^{-1}$) is the diffusion coefficient of methanol in the membrane.

The reference value of methanol diffusion coefficient in water in the void pores was taken to be $1.58 \times 10^{-5}\,\mathrm{cm}^2\,\mathrm{s}^{-1}$ at $T_{ref} = 298$ K. This value was corrected to the actual temperature using an exponential dependence:

$$D_M^w = 1.58 \times 10^{-5} \exp(0.026\,236(T - T_{\mathrm{ref}})) \tag{19}$$

where D_M^w (in $\mathrm{cm}^2\,\mathrm{s}^{-1}$) is the diffusion coefficient of methanol in water.

The profile of *hydraulic permeability* $K_p(x)$ is described in the following manner. K_p^{BL} is the hydraulic permeability of the backing layers and K_p^M is that of the membrane. We introduce a correction factor ε^M which is a volume fraction of membrane in the catalyst layer. Then

$$K_p = \begin{cases} K_p^{BL} & \text{in backing layers} \\ K_p^M \varepsilon^M & \text{in catalyst layers} \\ K_p^M & \text{in membrane} \end{cases} \tag{20}$$

The steps in the function (Equations 20) were smoothed to prevent formation of infinite gradients in the numerical algorithm.

The *electrokinetic permeability* of the membrane is K_φ^M. According to [7] this value in the catalyst layers should be corrected by multiplying by the volume fraction of membrane phase in these layers. We, therefore, have

$$K_\varphi = \begin{cases} K_\varphi^M \varepsilon^M & \text{in catalyst layers} \\ K_\varphi^M & \text{in membrane} \end{cases} \tag{21}$$

As in the case of K_p, the steps in Equations 21 were smoothed.

Binary diffusion coefficients were calculated using the approximation [10] with the correction for porosity ϵ:

$$D_{kl} \to \epsilon^{1.5} D_{kl} \tag{22}$$

The Knudsen diffusion coefficient was calculated using

$$D_k^K = \psi\langle r\rangle\sqrt{\frac{8RT}{\pi M_k}} \tag{23}$$

where T is absolute temperature, M_k molecular weight of kth component, $\langle r\rangle$ the mean pore radius and ψ a correction factor.

References

1. J. Wang and R.F. Savinell, 'Simulation Studies on the Fuel Electrode of a Methanol Air Polymer Electrolyte Fuel Cell'. *In*: S. Srinivasan, D.D. Macdonald and A.C. Khandkar (Eds.), *Proceedings of the Symposium on 'Electrode Materials and Processes for Energy Conversion and Storage'* (10 South Main St., Pennington, NJ 08534-2896, USA), (1994) pp. 326–44.
2. K. Scott, W. Taama and J. Cruickshank, *J. Power Sources* **65** (1997) 159–71.
3. K. Scott, W. Taama and J. Cruickshank, *J. Appl. Electrochem.* **28** (1998) 289–97.
4. T.E. Springer, T.A. Zavodzinski and S. Gottesfeld, *J. Electrochem. Soc.* **138**(8) (1991) 2334–42.
5. D.M. Bernardi and M.W. Verbrugge, *J. Electrochem. Soc.* **139**(9) (1992) 2477–91.
6. A.A. Kulikovsky, J. Divisek and A.A. Kornyshev, *J. Electrochem. Soc.* **147**(3) (2000) 953–9.
7. D.M. Bernardi and M.W. Verbrugge, *AIChE J.* **37**(8) (1991) 1151–63.
8. A.A. Kulikovsky, J. Divisek and A.A. Kornyshev *J. Electrochem. Soc.* **146**(11) (1999) 3981–91.
9. X. Ren, T.A. Zawodzinski Jr, F. Uribe, H. Dai and S. Gottesfeld, 'Methanol cross-over in direct methanol fuel cells'. In: *Electrochem. Soc. Proc.* **95-23** (1995) 284–98.
10. R.B. Bird, W.E. Stewart and E.N. Lightfoot ('Transport Phenomena') J. Wiley & Sons, New York, 1960) p. 503.